

## Scientific Article

# Identification of Induced Radionuclides Produced from Dental Metals in Proton Beam Therapy for Head and Neck Cancer



Ryohei Kato, MS,<sup>a,\*</sup> Takahiro Kato, PhD,<sup>a,b</sup> Yuki Narita, PhD,<sup>a</sup> Sho Sasaki, MS,<sup>a</sup> Kanako Takayama, DDS, PhD,<sup>c</sup> and Masao Murakami, MD, PhD<sup>c</sup>

<sup>a</sup>Department of Radiation Physics and Technology, Southern Tohoku Proton Therapy Center, Fukushima, Japan;

<sup>b</sup>Department of Radiological Sciences, School of Health Sciences, Fukushima Medical University, Fukushima, Japan; and

<sup>c</sup>Department of Radiation Oncology, Southern Tohoku Proton Therapy Center, Fukushima, Japan

Received 5 May 2022; accepted 11 December 2022

## Abstract

**Purpose:** To identify the induced radionuclides produced from dental metals in proton beam therapy and investigate the accuracy of the Monte Carlo (MC) simulation by comparing the measured radioactivity.

**Methods and Materials:** Two dental metals of pure titanium and gold-silver-palladium alloy, commonly used in Japan, were used in this study. The dental metal placed at the center of Spread-out Bragg Peak was irradiated by 150-MeV passive scattering proton beam. The gamma rays emitted from the activated dental metals were measured using a high purity germanium (HPGe) detector. The induced radionuclides were identified from the measured gamma-ray energies. Furthermore, the Particle and Heavy Ion Transport code System v.3.24 and DCHAIN were used for the MC simulation. The measured radionuclides and their radioactivity were compared with the simulation results.

**Results:** In the MC simulation for the activated titanium, vanadium-47, with a half-life of 32.6 minutes had the strongest radioactivity among the induced radionuclides. The energy peaks of gamma rays emitted from titanium-51, scandium-43, scandium-44, and annihilation gamma rays were observed for the activated titanium in the HPGe detector. In the MC simulation for the activated gold-silver-palladium alloy, silver-108, with a half-life of 2.4 minutes had the strongest radioactivity. The energy peaks of gamma rays emitted from silver-104, silver-104 m, silver-108, and annihilation gamma rays were observed for the activated gold-silver-palladium alloy in the HPGe detector. Furthermore, the induced radionuclides and their radioactivity in the MC simulation were consistent with the measurement results for both dental metals, except for a few radionuclides.

**Conclusions:** We identify the induced radionuclides produced from 2 dental metals and compared their radioactivity between the measurements and the MC simulation. Although the identification of the induced radionuclides using the MC simulation remains uncertain, the MC simulation can be clinically effective for pre-estimating the induced radionuclides in proton beam therapy.

© 2022 The Author(s). Published by Elsevier Inc. on behalf of American Society for Radiation Oncology. This is an open access article under the CC BY-NC-ND license (<http://creativecommons.org/licenses/by-nc-nd/4.0/>).

Sources of support: This work was supported by JSPS KAKENHI grant number JP20K16775.

Disclosures: The authors declare that they have no known competing financial interests or personal relationships that could have appeared to influence the work reported in this paper.

Research data are stored in an institutional repository and will be shared upon request to the corresponding author.

\*Corresponding author: Ryohei Kato, MS; E-mail: [ryo.kato3511@gmail.com](mailto:ryo.kato3511@gmail.com)

<https://doi.org/10.1016/j.adro.2022.101153>

2452-1094/© 2022 The Author(s). Published by Elsevier Inc. on behalf of American Society for Radiation Oncology. This is an open access article under the CC BY-NC-ND license (<http://creativecommons.org/licenses/by-nc-nd/4.0/>).

## Introduction

Proton beam therapy (PBT) has advantages, such as the sharp lateral penumbra and steep distal fall-off at the end of its range, compared with conventional x-ray therapy. Using these physical characteristics, PBT offers a

superior dose concentration for targets and can avoid delivering doses to critical organs. Recently, besides the conventional passive scattering PBT, new irradiation techniques, such as pencil beam scanning (PBS) method, have been developed, and the indications for PBT are increasing.<sup>1,2</sup> Head and neck (H&N) cancer is a good indication for PBT because some critical organs are adjacent to the target.<sup>3</sup>

H&N cancer patients often have dental metals such as an implant or a crown in their oral cavity. Although dental metals in the oral cavity are basically removed before treatment planning, they are often irremovable. In such cases, the proton field should be arranged to avoid the metal. However, it is often difficult to avoid irradiation due to geometric and anatomic limitations. If the proton beam passes through these metals, the dose distribution is largely perturbed by the metal.<sup>4-10</sup> Moreover, high-Z metals can be radioactivated by protons or secondary neutrons in PBT. Radioactivation may increase radiation exposure in patients and therapy staff.<sup>11</sup> In PBT, particularly passive scattering PBT, patient-specific devices, such as a range compensator and a brass collimator, are often used. Therefore, the radioactivation effects of induced radionuclides and their radiation exposure have been investigated.<sup>12,13</sup> These studies report the radioactivation of materials outside the human body. However, the radioactivation effect caused by materials inside the human body, such as dental metal, is yet to be clarified. In the conventional x-ray therapy, severe oral mucositis adjacent to dental metals was reported because of backscatter radiations.<sup>14,15</sup> Although the backscatter radiation in PBT is less of an issue than that of x-ray therapy, the dose delivered to the mucosa adjacent to the dental metal can increase because of radiation, such as beta rays and Auger electrons, emitted from the activated metal. Therefore, the radioactivation effects of the metal should be investigated. Generally, a high purity germanium (HPGe) detector is used to evaluate the radioactivation by counting the emitted gamma rays. However, it is difficult to obtain dental materials of appropriate sizes and shapes, and the overwhelming majority of radiation therapy facilities do not have the HPGe detector. Therefore, the Monte Carlo (MC) simulation can be clinically effective for estimating the induced radionuclides. In this study, we aimed to identify the induced radionuclides produced from dental metals using the MC simulation and measurement from an HPGe detector. Additionally, we also discussed the accuracy and issues of the MC simulation for evaluating the radioactivation.

## Methods and Materials

### Characteristics of dental metals

Two dental metals of JIS type 2 pure titanium (GC, Tokyo, Japan) and 12% gold-silver-palladium alloy (YAMAKIN, Osaka, Japan) commonly used in Japan

were used in this study. Dental treatment using these metals is covered by public insurance in Japan, and these metals are generally used in dental materials. Titanium is used for crowns and implants, and gold-silver-palladium alloy is mainly used for crowns and inlays. These metals are processed for each patient. The unprocessed sizes of titanium and gold-silver-palladium alloy supplied by the manufacturer were  $\varphi 1.6 \times 1.5$  cm and  $1.3 \times 0.6 \times 0.2$  cm, respectively.

### Identification of radionuclides

The induced radionuclides produced from the dental metals caused by the proton beam irradiation were identified using the MC simulation and the measurement of the HPGe detector. The dental metal was irradiated by a 150-MeV proton beam with a 60-mm Spread-out Bragg Peak (SOBP) size. We used a passive scattering PBT system, the treatment machine of Proton Type (Hitachi, Tokyo, Japan), at our institution. This machine consists of a wobbling magnet, scatterer, primary and secondary collimator, monitor chamber, and multileaf collimator. An initial proton energy of 150-MeV is often selected for patients with H&N cancer at our institution. Additionally, a proton beam with a 60-mm SOBP is frequently used for patients with H&N cancer. Therefore, this beam parameter was selected in this study. The dental metal was placed at an isocenter, the center of SOBP, in a water phantom of  $20 \times 20 \times 20$  cm. Here, the PBT for H&N cancer, including the reirradiation, is actively performed at our institution.<sup>16-19</sup> From our experience, the dental metal often exists within the SOBP region. As mentioned previously, the dental metal is removed before PBT. If the dental metal is not removed, proton fields include dental metals occasionally in PBT for patients with H&N cancer, such as maxillary sinus, gingival, and tongue cancer. Dental metals can be irradiated in the SOBP region in maxillary sinus and gingival cancer. Also, dental metals often exist at the proximal or distal side of the SOBP region in tongue cancer. Therefore, the SOBP center was considered an appropriate measurement point. The field size was  $10 \times 10$  cm at the isocenter. The dose delivered to the isocenter was 5 Gy. Under irradiation conditions, the induced radionuclides and their radioactivity were compared with the MC simulation and measurement.

The radioactivation of 2 dental metals was calculated using the Particle and Heavy Ion Transport code System v.3.24<sup>20</sup> and DCHAIN-SP 2014.<sup>21</sup> The DCHAIN specification manual describes that DCHAIN estimates induced radionuclides and their radioactivity by adding nuclide production rates of neutrons below 20 MeV that were calculated from cross-section library and those of protons, heavy ions, mesons, and high energy neutrons above 20

MeV. In the MC simulation, nuclear interactions of protons and secondary neutrons were simulated using the Liège intranuclear cascade model<sup>22,23</sup> and JENDL-4.0 neutron cross section library,<sup>24</sup> respectively. The phase space information obtained from the preliminarily full MC simulation of our treatment nozzle was used for estimating the radioactivation, which included protons as well as other particles, such as photons, electrons, positrons, and neutrons. Subsequently, the delay time from the end of the irradiation in the measurement was accounted for in DCHAIN.

Measurement using the HPGe detector was conducted under the same conditions as the MC simulation. The HPGe detector used in this study was a GEM20P4-70 coaxial detector system (ORTEC, Oak Ridge, Tennessee, USA). Two and a half minutes after the end of the proton beam irradiation, gamma rays emitted from the activated metal were counted using the HPGe detector. The background obtained from nonactivated metal was subtracted from the gamma-ray spectrum of the activated metal. The induced radionuclides were identified based on the measured gamma-ray energies. The radioactivity was given by:

$$A = \frac{N_C \lambda t_m}{\varepsilon \gamma (1 - e^{-\lambda t_m})},$$

where A is radioactivity,  $N_C$  is photo peak count rates,  $\varepsilon$  is detection efficiency in the gamma-ray energy,  $\gamma$  is energy intensity of the emitted gamma-ray,  $\lambda$  is the decay constant of the radionuclide, and  $t_m$  is measurement time. The detection efficiency of the gamma-ray energies in the induced radionuclides was determined based on measurements of some standard sources.<sup>25,26</sup> The radioactivity in the measurement was compared with the results of the MC simulation.

## Results

### Identification of radionuclides

In the MC simulation, the 10 induced radionuclides with the high radioactivity produced from the titanium and gold-silver-palladium alloy by the proton beam irradiation are shown in Tables 1 and 2, respectively. In Table 1, vanadium-47 with a half-life of 32.6 minutes had the strongest radioactivity among the induced radionuclides. The induced radionuclides, such as scandium-44 and scandium-43, had a relatively long half-life of approximately 4 hours among the simulation result. Moreover, since most of these induced radionuclides had  $\beta^+$  decay and electron capture decay, a large number of annihilation gamma rays would be emitted from the titanium. The total specific radioactivity in the titanium was  $1.1 \times 10^3$  Bq per cc. In the measurement, the strong energy peaks in channels of 511 and 1157 keV were observed in the gamma-ray spectra of the activated titanium (Fig. 1). The energy peak at 1157 keV was estimated to be the gamma ray emitted from scandium-44 compared with Table 1. The peak at 511 keV was that of the annihilation gamma ray. Furthermore, the energy peaks, such as scandium-42 m, scandium-43, titanium-51, and vanadium-47, were observed in comparison with Table 1. However, the energy peaks, such as oxygen-15, scandium-46 m, oxygen-14, and scandium-49, were not observed because of the weak radioactivity or background.

In Table 2, many radioisotopes of silver were produced by the proton beam irradiation, and silver-108, with a half-life of 2.4 minutes, had the strongest radioactivity. Among these induced radionuclides, cadmium-105 and cadmium-104 had a relatively long half-life of approximately 1 hour. The intensity of the annihilation gamma ray would be strong as well as those of the activated titanium because

**Table 1** Induced radionuclides generated from titanium in the Monte Carlo simulation

Radionuclides	Activity (Bq)	Decay mechanism	Half-life (min)	Gamma-ray energy (keV) and intensities
V-47	1.91E+03	EC $\beta^+$	32.6	1793.9 (0.2%)
Ti-45	3.67E+02	EC $\beta^+$	184.8	719.6 (0.2%)
O-15	2.77E+02	$\beta^+$	2.0	-
Sc-46 m	1.24E+02	IT	0.3	142.5 (62.0%)
Sc-44	1.01E+02	EC $\beta^+$	238.2	1157.0 (99.9%), 1499.5 (0.9%)
O-14	8.91E+01	$\beta^+$	1.2	2312.6 (99.4%)
Sc-42 m	6.53E+01	EC $\beta^+$	1.0	437.5 (100%), 1227.0 (99.0%), 1524.5 (99.7%)
Sc-49	6.42E+01	$\beta^-$	57.2	1761.9 (0.05%)
Ti-51	5.71E+01	$\beta^-$	5.76	320.1 (93.1%), 608.6 (1.2%), 928.6 (6.9%)
Sc-43	4.20E+01	EC	233.5	372.9 (22.5%)

Abbreviations: EC = electron capture; IT = isomeric transition; MC = Monte Carlo.

**Table 2** Induced radionuclides generated from gold-silver-palladium alloy in the Monte Carlo simulation

Radionuclides	Activity (Bq)	Decay mechanism	Half-life (minutes)	Gamma-ray energy (keV) and intensities
Ag-108	4.64E+03	$\beta^-$ , EC $\beta^+$	2.4	633.0 (1.8%), 434.0 (0.5%), 618.9 (0.3%)
Ag-105 m	7.23E+02	EC, IT	7.2	319.2 (0.2%)
Cu-62	6.58E+02	EC $\beta^+$	9.7	875.7 (0.2%), 1173.0 (0.3%)
Ag-110	5.80E+02	$\beta^-$ , EC	0.41	657.5 (4.5%)
Ag-106	3.28E+02	$\beta^-$ , EC $\beta^+$	24	511.9 (17.0%), 622.0 (0.3%), 873.5 (0.2%)
Cd-105	1.62E+02	EC	55.5	346.9 (4.2%), 607.2 (3.7%), 961.8 (4.7%)
Ag-104 m	1.36E+02	EC $\beta^+$ , IT	33.5	555.8 (90.0%), 1238.8 (3.9%), 2276.7 (2.4%)
Ag-107 m	1.27E+02	IT	0.74	93.1 (4.7%)
Cd-103	8.19E+01	EC $\beta^+$	7.3	1079.9 (5.0%), 1448.7 (5.1%), 1461.8 (10.8%)
Cd-104	7.77E+01	EC	55.7	83.5 (47.0%), 559.0 (6.3%), 709.3 (19.5%)

Abbreviations: EC = electron capture; IT = isomeric transition; MC = Monte Carlo.

these induced radionuclides have  $\beta^+$  and electron capture decay. The total specific radioactivity in the gold-silver-palladium alloy was  $3.9 \times 10^5$  Bq per cc. In the measurement, the strong energy peaks in channels of 511, 556, 633, and 768 keV were observed in the gamma-ray spectra of the activated gold-silver-palladium alloy (Fig. 2). The energy peaks at 556, 633, and 768 keV were estimated using the gamma rays emitted from silver-104m and silver-108 compared with Table 2. The peak at 511 keV was that of the annihilation gamma ray. Further, the energy peaks of silver-102, silver-106, silver-110, cadmium-103, and cadmium-104 were observed in comparison with Table 2. However, the energy peaks of silver-105m, copper-62, cadmium-105, and silver-107m were not observed because of the weak radioactivity or background.

### Comparison of induced radionuclides and their radioactivity between MC simulation and measurement

It was revealed that induced radionuclides and their radioactivity from the titanium in the measurement were identified by comparing them with MC simulation results (Table 3). The radioactivity in scandium-43 and scandium-44 was consistent in measurement and MC simulation, and errors were within 4% and 13%, respectively. Also, some peaks could not be observed because of backgrounds and weak radioactivity. Table 4 shows the induced radioactivity in the activated gold-silver-palladium alloy between the MC simulation and measurement. The radioactivity in silver-104m and silver-104 were

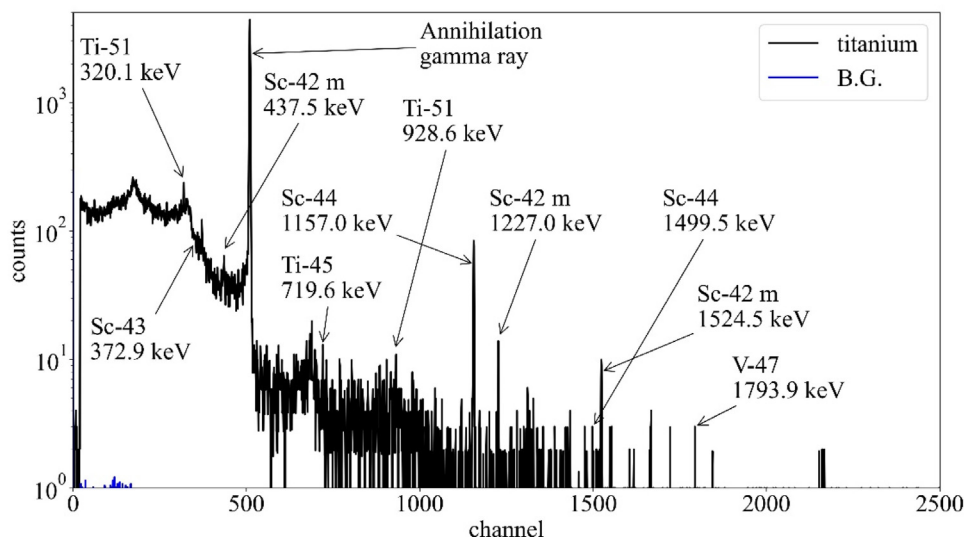


**Figure 1** Gamma-ray spectra of the activated titanium measured by the high purity germanium detector after 2.5 minutes of the irradiation. Arrows showed radionuclides predicted by the Monte Carlo simulation (listed in Table 1). Abbreviation: BG = background.

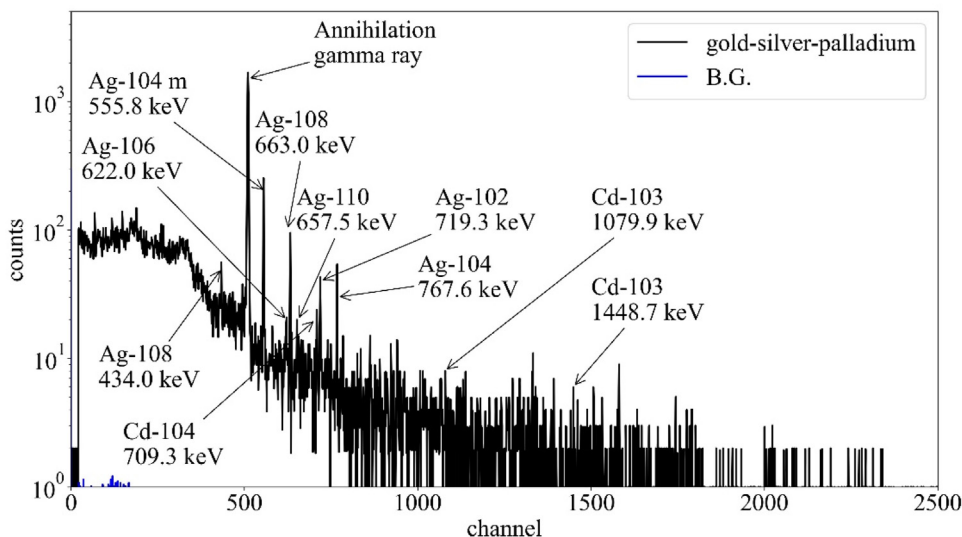


**Figure 2** Gamma-ray spectra of the activated gold-silver-palladium alloy measured by the high purity germanium detector after 2.5 minutes of the irradiation. Arrows showed radionuclides predicted by the Monte Carlo simulation (listed in Table 2). Abbreviation: BG = background.

**Table 3** Comparison of radioactivity between measurements and the MC simulation in the activated titanium

Radionuclides	Radioactivity (Bq)	
	Measurement	MC
Ti-51	36.2 (320.1 keV), - (928.6 keV)	57.1
Sc-43	43.7 (372.9 keV)	42.0
Sc-42m	12.2 (437.5 keV), - (1227.0 keV), - (1524.5 keV)	65.3
Sc-44	104.2 (1157.0 keV), - (1499.5 keV)	100.8
V-47	- (1793.9 keV)	191.7

Abbreviation: MC = Monte Carlo.

consistent, and errors were within 13% and 8%, respectively. However, the silver-108 radioactivity was observed to have a difference of approximately twice between the measurement and the MC simulation. Some peaks could not be observed because of backgrounds and weak radioactivity. Also, since the gamma ray of 511.9 keV emitted from silver-104m had close energy to that of the annihilation gamma ray, a strong energy peak in the channel of 511 keV was observed in the measurement.

### Discussion

In this study, we identified the induced radionuclides produced from the dental metals, commonly used in Japan, in PBT. Energy peaks observed in the HPGe detector were in line with the simulation results except for a few induced radionuclides. The radioactivity of a few radionuclides was consistent between the measurement

**Table 4** Comparison of radioactivity between measurements and the Monte Carlo simulation in the activated gold-silver-palladium alloy.

Radionuclides	Radioactivity (Bq)	
	Measurement	MC
Ag-108	2216.5 (434.0 keV), 2430.8 (633.0 keV)	4640.9
Ag-104m	153.9 (555.8 keV)	135.7
Ag-106	- (622.0 keV)	327.8
Ag-110	- (657.5 keV)	589.0
Cd-104	120.6 (709.3 keV)	77.7
Ag-102	49.1 (719.3 keV)	11.9
Ag-104	60.4 (767.6 keV)	65.4
Cd-103	- (1079.9 keV), - (1448.7 keV)	81.9

Abbreviation: MC = Monte Carlo.

and the MC simulation by approximately 10%; however, that of some radionuclides deviated largely. The measurement using the HPGe detector has some uncertainties, such as a background and lack of gamma-ray counts. Also, the intranuclear cascade model in Particle and Heavy Ion Transport code System was known to have several discrepancies for low-energy (below 100 MeV) proton incident reactions.<sup>23</sup> In summary, the evaluation of radionuclide production using the MC simulation is limited to the accuracy of the reaction model. Since the accuracy of reactions between metals, such as Ti, Ag, Au, and Pd, and protons is unclear, the MC simulation may include some uncertainties. Therefore, it is necessary to

improve the estimation accuracy by combining the MC simulation and the measurement. However, the actual dental material may not be available for the measurement, and most radiation therapy facilities do not have a HPGe detector. Therefore, pre-estimating the induced radionuclides using the MC simulation is clinically a safe and beneficial method.

The report of task group 136 of the American Association of Physicists in Medicine proposed to survey activated materials routinely and dispose or recycle the patient-specific consumable components after completing the course of PBT and decay to the background has occurred.<sup>11</sup> Additionally, although handling of the activated material on the proton beam lines, such as the range compensator and the brass collimator, has been discussed,<sup>12,13</sup> the effect of the activation of metals inside the human body, such as dental metal, has not been clarified in PBT and is not specified in the guideline. In the present study, we revealed that the induced radionuclides with half-lives of several hours were produced from the dental metals commonly used in Japan. The effects of the metals inside the human body on clinical outcomes are still unknown in PBT. Therefore, further research on the induced radionuclides' clinical effects is needed. There is still room for improvement in a more accurate evaluation; however, we believe that this study can help handle the standardization of these metals in PBT.

In this study, we investigated the radioactivation of the 2 metals commonly used in Japan for dental treatment. Various other dental materials, such as amalgams and composite resin were also investigated, and the radioactivation of these materials is also unclear. Since our results indicate that the MC simulation is a useful tool, the radioactivation of these materials should be further evaluated in the future. Moreover, the metal size used in this study is different from that attached to the patient's teeth. Since the dental metal is manufactured and casted, the metal size and shape vary for each patient. In this study, the dental metal radioactivation before manufacturing was verified to eliminate uncertainties of the size and shape. Although the radioactivity changes depending on the metal's size and shape, we considered that the evaluation was overestimated (clinically safe side) because the metal size used in this study is larger than that after processing. Verifications of the radioactivation using an H&N phantom would be required to simulate more realistic clinical scenario. Additionally, since the size and shape of the 2 dental metals were different, the specific radioactivity was compared. In fact, it is important to discuss doses, and the conversion from the specific radioactivity to doses is an important issue. However, few studies have reported the radioactivation of the dental metal in PBT. Thus, in this study, we focused on the identification of induced radionuclides and the usefulness of the MC simulation. Evaluating the radioactivation with doses is an important issue that should be addressed in the future. The specific

radioactivity in the gold-silver-palladium alloy was larger than that in the titanium, so the activated gold-silver-palladium alloy should be carefully handled.

The clinical effects of the activated metals on patients could not be sufficiently evaluated in this study. In x-ray therapy, severe oral mucositis adjacent to dental metals was reported because of backscatter radiations from the metal.<sup>14,15</sup> Çatli reported that the dose increases to 2 mm in front of various dental implants because of the backscatter radiation in 6 MV photons when analyzed using MC simulation.<sup>27</sup> According to this report, however, it is unclear whether dose increases because of the backscatter radiations cause increased mucositis. Many risk factors have been identified for radiation-induced mucositis, including chemotherapy, bad oral hygiene, and smoking.<sup>28</sup> Therefore, it is difficult to associate mucositis with the effects of dental metals in x-ray therapy. Although the mucosal dose enhancement adjacent to dental metals caused by the radioactivation is concerned in PBT, there are no reports on this issue. Therefore, the dental metal radioactivation in PBT may also be a risk factor for mucositis. In the present study, we clarified the induced radionuclides produced from the dental metals; however, the clinical effects caused by these induced radionuclides are unclear. Therefore, further research is required on the induced radionuclides' clinical effects in PBT.

This study was conducted under limited conditions. Measurements using the PBS system may be appropriate to more comprehensively evaluate the radioactivation. Recently, the PBS system has become more mainstream than the passive scattering system. There are few neutron contaminations in the PBS system. Moreover, avoiding metals is easy from proton beam fields, especially in intensity modulated proton therapy. Therefore, the dental metal radioactivation problem may be less likely to occur with the PBS system than with passive scattering. However, we speculate that it will be difficult to completely avoid metals even when using the PBS system, if the tumor is in contact with the dental metal, or if a portion of the metal is embedded in the tumor. Besides, it may be more difficult to avoid metal, particularly for reirradiation cases, because of the limited beam arrangement. In this study, we aimed to evaluate radioactivation and to investigate the usefulness of the MC simulation. This research requires having the HPGe detector. Fortunately, the HPGe detector is available at our institution, enabling us to conduct this research. Although we used the passive scattering system, we believe that our results are helpful for the PBS system. Additionally, we evaluated the radioactivation only in a certain proton beam setting since this study focused on dental metals existing the oral cavity. The anatomic position of dental metals is around a few centimeters from the body surface. Therefore, we determined that the measurement point is the center at the 150-MeV initial proton beam with the 60-mm SOBPs size. However, the radioactivation by higher energy proton

beams is a very interesting issue. We would like to evaluate a comprehensive verification of the energy dependence of the radioactivation in the near future.

## Conclusions

In this study, we identified the induced radionuclides produced from 2 dental metals of titanium and gold-silver-palladium alloys in PBT and verified the accuracy of the MC simulation. The half-lives of radionuclides were below several hours, so most of them decayed quickly. Additionally, their radioactivity between the MC simulation and the measurement was consistent in a few radionuclides. Although the evaluations of the radioactivation of the metal inside the human body using the MC simulation remain uncertain, the MC simulation is a clinically safe and effective method for pre-estimating the induced radionuclides in PBT.

## Acknowledgments

We would like to thank operator staffs of Hitachi for supporting the measurement.

## References

- Olsen DR, Bruland OS, Frykholm G, Norderhaug IN. Proton therapy – A systematic review of clinical effectiveness. *Radiother Oncol.* 2007;83:123-132.
- Mohan R, Grosshans D. Proton therapy – Present and future. *Adv Drug Deliv Rev.* 2017;109:26-44.
- Blanchard P, Gunn GB, Lin A, Foote RL, Lee NY, Frank SJ. Proton therapy for head and neck cancers. *Semin Radiat Oncol.* 2018;28:53-63.
- Newhauser WD, Koch NC, Fontenot JD, et al. Dosimetric impact of tantalum markers used in the treatment of uveal melanoma with proton beam therapy. *Phys Med Biol.* 2007;52:3979-3990.
- Newhauser W, Fontenot J, Koch N, et al. Monte Carlo simulations of the dosimetric impact of radiopaque fiducial markers for proton radiotherapy of the prostate. *Phys Med Biol.* 2007;52:2937-2952.
- Carnicer A, Angellier G, Theriat J, Sauerwein W, Caujolle JP, Hérault J. Quantification of dose perturbations induced by external and internal accessories in ocular proton therapy and evaluation of their dosimetric impact. *Med Phys.* 2013;40: 061708.
- Verburg JM, Seco J. Dosimetric accuracy of proton therapy for chordoma patients with titanium implants. *Med Phys.* 2013;40: 071727.
- Dietlicher I, Casiraghi M, Ares C, et al. The effect of surgical titanium rods on proton therapy delivered for cervical bone tumors: experimental validation using an anthropomorphic phantom. *Phys Med Biol.* 2014;59:7181-7194.
- Jia Y, Zhao L, Cheng C-W, McDonald MW, Das IJ. Dose perturbation effect of metallic spinal implants in proton beam therapy. *J Appl Clin Med Phys.* 2015;16:333-343.
- Oancea C, Shipulin K, Mytsin G, et al. Effect of titanium dental implants on proton therapy delivered for head tumors: Experimental validation using an anthropomorphic head phantom. *J Instrum.* 2017;12:C03082.
- Thomadsen B, Nath R, Bateman FB, et al. Potential hazard due to induced radioactivity secondary to radiotherapy: The report of task group 136 of the American Association of Physicists in Medicine. *Health Phys.* 2014;107:442-460.
- Cesana A, Mauro E, Silari M. Induced radioactivity in a patient-specific collimator used in proton therapy. *Nucl Instrum Methods Phys Res B.* 2010;268:2272-2280.
- Lee SH, Cho S, You SH, et al. Evaluation of radioactivity induced by patient-specific devices in proton therapy. *J Korean Phys Soc.* 2012;60:125-128.
- Farahani M, Eichmiller FC, McLaughlin WL. Measurement of absorbed doses near metal and dental material interfaces irradiated by x- and gamma-ray therapy beams. *Phys Med Biol.* 1990;35:369-385.
- Ravikumar M, Ravichandran R, Sathiyam S, Supe SS. Backscattered dose perturbation effects at metallic interfaces irradiated by high-energy X- and gamma-ray therapeutic beams. *Strahlenther Onkol.* 2004;180:173-178.
- Nakamura T, Azami Y, Ono T, et al. Preliminary results of proton beam therapy combined with weekly cisplatin intra-arterial infusion via a superficial temporal artery for treatment of maxillary sinus carcinoma. *Jpn J Clin Oncol.* 2016;46:46-50.
- Endo H, Takayama K, Mitsudo K, et al. Proton beam therapy in combination with intra-arterial infusion chemotherapy for T4 squamous cell carcinoma of the maxillary gingiva. *Cancers.* 2018;10:333.
- Takayama K, Nakamura T, Takada A, et al. Treatment results of alternating chemoradiotherapy followed by proton beam therapy boost combined with intra-arterial infusion chemotherapy for stage III–IVB tongue cancer. *J Cncer Res Clin Oncol.* 2016;142:659-667.
- Hayashi Y, Nakamura T, Mitsudo K, et al. Re-irradiation using proton beam therapy combined with weekly intra-arterial chemotherapy for recurrent oral cancer. *Asia Pac J Clin Oncol.* 2017;13:e394-e401.
- Sato T, Iwamoto Y, Hashimoto S, et al. Features of Particle and Heavy Ion Transport code System (PHITS) version 3.02. *J Nucl Sci Technol.* 2018;55:684-690.
- Ratliff HN, Matsuda N, Abe S, et al. Modernization of the DCHAIN-PHITS activation code with new features and updated data libraries. *Nucl Instrum Methods Phys Res B.* 2020;484:29-41.
- Boudard A, Cugnon J, David J-C, Leray S, Mancusi D. New potentialities of the Liège intranuclear cascade model for reactions induced by nucleons and light charged particles. *Phys Rev C.* 2013;87: 014606.
- Iwamoto Y, Sato T, Hashimoto S, et al. Benchmark study of the recent version of the PHITS code. *J Nucl Sci Technol.* 2017;54:617-635.
- Shibata K, Iwamoto O, Nakagawa T, et al. JENDL-4.0: A new library for nuclear science and engineering. *J Nucl Sci Technol.* 2011;48:1-30.
- Ewa IO, Bodizs D, Czifrus S, Molnar Z. Monte Carlo determination of full energy peak efficiency for a HPGe detector. *Appl Radiat Isot.* 2001;55:103-108.
- Hurtado S, García-León M, García-Tenorio R. Monte Carlo simulation of the response of a germanium detector for low-level spectrometry measurements using GEANT4. *Appl Radiat Isot.* 2004;61:139-143.
- Çatli S. High-density implants and radiotherapy planning: Evaluation of effects on dose distribution using pencil beam convolution algorithm and Monte Carlo method. *J Appl Clin Med Phys.* 2015;16:46-52.
- Maria OM, Eliopoulos N, Muanza T. Radiation-induced oral mucositis. *Front Oncol.* 2017;7:89.